Cyclic MrIA: A Stable and Potent Cyclic Conotoxin with a Novel Topological Fold that Targets the Norepinephrine Transporter

Erica S. Lovelace, Christopher J. Armishaw, Michelle L. Colgrave, Maria E. Wahlstrom, Paul F. Alewood, Norelle L. Daly, and David J. Craik*

Institute for Molecular Bioscience, University of Queensland, Brisbane, Queensland 4072, Australia

Received March 16, 2006

Conotoxins, disulfide-rich peptides from the venom of cone snails, have created much excitement over recent years due to their potency and specificity for ion channels and their therapeutic potential. One recently identified conotoxin, MrIA, a 13-residue member of the χ-conotoxin family, inhibits the human norepinephrine transporter (NET) and has potential applications in the treatment of pain. In the current study, we show that the β-hairpin structure of native MrIA is retained in a synthetic cyclic version, as is biological activity at the NET. Furthermore, the cyclic version has increased resistance to trypsin digestion relative to the native peptide, an intriguing result because the cleavage site for the trypsin is not close to the cyclization site. The use of peptides as drugs is generally hampered by susceptibility to proteolysis, and so, the increase in enzymatic stability against trypsin observed in the current study may be useful in improving the therapeutic potential of MrIA. Furthermore, the structure reported here for cyclic MrIA represents a new topology among a growing number of circular disulfide-rich peptides.

Introduction

Conotoxins are peptide toxins derived from cone snails that vary in length from about 10 to 30 residues[1−3] and act on a wide range of ion channels. Cone snail-derived toxins have been under investigation in recent years for the treatment of many diseases and conditions, including chronic pain, epilepsy, cardiovascular disease, psychiatric disorders, Parkinson's disease, Alzheimer's disease, cancer, and stroke.[4−8] In addition to their therapeutic applications, conotoxins have been widely studied due to their convenient chemical synthesis and have proved useful as pharmacological probes because of their high potency and specificity at various ion channels. On the basis of the large number of *Conus* species and the numerous conotoxins found in a single species, it has been suggested that there are at least 50 000 different conotoxins[3], making them a rich source of bioactive molecules.

The disulfide connectivity and pharmacological activities of conotoxins have been used to divide them into a number of families (e.g., α, δ, μ, χ, ω, ρ, τ, σ, and κ).[1,2] Several conotoxins are currently in clinical trials, and one member of the ω-conotoxin family, MVIIA (Prialt), is on the market for the treatment of chronic pain.[9,10] In addition, two closely related χ-conotoxins, MrIA and MrIB, isolated from *Conus marmoreus*, are selective inhibitors of the norepinephrine transporter (NET[a]),[11,12] and a derivative of MrIA is currently being investigated as an analgesic agent.[13] Drugs that inhibit the NET also have the potential to treat a number of neurological conditions, including depression,[14] anxiety,[15] chronic pain,[16,17] and other psychiatric disorders,[18] as well as influencing learning, memory, endocrine, and autonomic functions.[19]

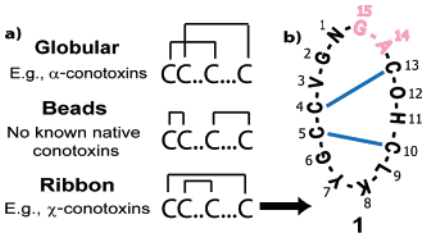

Figure 1. Schematic representation of (a) the three possible types of disulfide connectivities with four cysteines: ribbon, globular, and beads and (b) the sequence of **1** with the ribbon connectivity.

MrIA[11,20,21] is a 13-residue peptide containing two disulfide bonds arranged in a "ribbon" (i.e., $Cys^{I}-Cys^{IV}$, $Cys^{II}-Cys^{III}$) connectivity in contrast to the "globular" ($Cys^{I}-Cys^{III}$, $Cys^{II}-Cys^{IV}$) connectivity observed in α and ρ conotoxins,[11] as shown in Figure 1a. The third possible disulfide connectivity, the "beads" isomer,[22] has not been found in native conotoxins. The three-dimensional structure of MrIA consists primarily of a β-hairpin, which places the N- and C-termini in close proximity.[23] The residues in the turn connecting the well-defined β-strands have been implicated as being important for biological activity, and the C-terminally amidated form, $MrIA-NH_2$, has been shown to be slightly more active than the native peptide.[12]

The inherent vulnerability to enzymatic cleavage and poor stability is one challenge that potentially limits the pharmaceutical use of peptides. Although most conotoxins are generally considered to be relatively stable due to their cross-bracing disulfide bond scaffold, improvements in stability can still be beneficial, such as in the case of MrIA, where a derivative, Xen2174, has been developed to overcome the relatively poor stability of the native peptide.[13] An alternative method of improving stability is by joining the N- and C-termini of the backbone via peptidic "linkers" to form a cyclic backbone. A similar approach has been tried on larger proteins, including β-lactamase,[24] the replicative helicase from *E. coli*, DnaB,[25] and

* Corresponding author. E-mail: d.craik@imb.uq.edu.au. Tel.: +61 7 3346 2019. Fax: +61 7 3346 2029.

[a] Abbreviations: NET, norepinephrine transporter; **1**, cyclic MrIA; Dnp, 2,6-dinitrophenyl; HBTU, 2-((1H)-benzotriazol-1-yl)-1,1,3,3,-tetramethyluronium hexafluorophosphate; MESNA, 2-mercaptoethanesulfonic acid sodium salt; PAM, phenylacetomidomethyl; TOCSY, 2D total correlation spectroscopy; NOE, nuclear Overhauser effect; NOESY, NOE spectroscopy; DQF-COSY, double quantum filtered correlation spectroscopy; ECOSY, exclusive correlation spectroscopy; WATERGATE, water suppression by gradient-tailored excitation; RMSD, root-mean-square deviation; RP-HPLC, reverse-phase high performance liquid chromatography; LCMS, liquid chromatography mass spectrometry; HF, anhydrous hydrogen fluoride; TFA, trifluoroacetic acid.

10.1021/jm060299h CCC: $33.50
Published on Web 10/07/2006

green fluorescent protein, with increases in stability observed upon cyclization.[26] The use of cyclization for enhanced stability has also been exemplified for the α-conotoxin MII.[27] In the current study, we show that this approach is also applicable for the χ-conotoxin, MrIA, despite the vastly different biological targets and structures of the α- and χ-conotoxins. A cyclic version of MrIA, with a two-residue linker, as shown in Figure 1b, was synthesized, and its solution structure and biological activity were determined. The cyclic molecule has substantially increased resistance to proteolysis relative to the native peptide but maintains equivalent biological activity.

Materials and Methods

Solid-Phase Peptide Synthesis. Boc-glycine-OCH_2 phenylacetomidomethyl (PAM) resin was obtained from Applied Biosystems (Foster City, CA). Boc-L-amino acid derivatives were purchased from Novabiochem (Laufelfingen, Switzerland). HBTU was obtained from Fluka (Büchs, Switzerland). *S*-Tritylmercaptopropionic acid was purchased from Peptides International (Louisville, KY). Dichloromethane, dimethylformamide, diisopropylethylamine, and trifluoroacetic acid (TFA) were of peptide synthesis grade and purchased from Auspep (Melbourne, Australia). Triisopropylsilane, *p*-cresol, ninhydrin, and 2-mercaptoethanesulfonic acid sodium salt (MESNA) were purchased from Aldrich (Milwaukee, WI). Hydrogen fluoride was from Matheson (La Porte, TX), and all other gases were purchased from BOC (Brisbane, Australia) and were of high purity grade. HPLC grade acetonitrile was from Merck (Melbourne, Australia), and HPLC-grade diethyl ether was from Fluka. Milli-Q distilled and deionized water were used.

Peptides were synthesized on a 0.25 mmol scale using Boc in situ neutralization protocols, using HBTU-mediated couplings.[28] The linear thioester peptide precursors were assembled manually using a *S*-tritylmercaptopropyl spacer attached to Boc-Gly-OCH_2 PAM resin. Removal of the *S*-trityl group was achieved using 5% triisopropylsilane in TFA (2 × 1 min), and the C-terminal amino acid amino acid was coupled with HBTU. Cleavage of the peptides from the resin was achieved by treatment with HF/*p*-cresol for 2 h at 0 °C. Following evaporation of the HF in vacuo, the crude peptides were precipitated with cold diethyl ether, filtered, washed with additional ether, then dissolved away from the resin using 50% aqueous acetonitrile/0.1% TFA, and lyophilized. The crude linear thioester peptides were purified using preparative RP-HPLC.

Cyclization. Linear thioester precursors were dissolved in aqueous buffer consisting of 6 M guanidine hydrochloride/0.1 M tris, pH 7.8, containing 1 mg/mL MESNA. The buffer was degassed with argon prior to the addition of the peptide, and all operations were performed under a blanket of argon. The reactions were monitored by analytical RP-HPLC. Reduced cyclic peptide was isolated by semipreparative RP-HPLC.

Oxidation. Cyclic MrIA, referred to as **1**, was oxidized by stirring the cyclic reduced peptide in 0.1 M NH_4HCO_3/50% 2-propanol, pH 8.0, in an open vessel and monitored by RP-HPLC and LC-MS. The mixture was acidified to pH 2 using TFA, the 2-propanol was evaporated in vacuo, and the final peptide product was isolated using semipreparative RP-HPLC.

Radioligand Binding Assays. Cos-7 cells grown in 150 mm dishes containing Dulbecco's modified eagle medium and 10% serum, were transiently transfected with plasmid DNA encoding hNET using a metafectene reagent (Biontex). Membrane was prepared 48 h post-transfection with the membrane stored in 10% glycerol at −80 °C. Tris (20 mM, pH 7.4), containing 75 mM NaCl, 0.2 mM EDTA, 0.2 mM EGTA, and 0.1% BSA, was used as the buffer for radioligand binding assays. [*N*-methyl ^{3}H] nisoxetine HCl (Perkin-Elmer Life Sciences, specific activity 70−87 Ci/mmol) was used at a concentration of 4.3 nM (approximate K_D value). The initial concentration of **1** was 3×10^{-5} M (for a final concentration of 1×10^{-5} M). Serial dilutions of 6 × 1:10 were then performed (50 μL top dose added to 450 μL buffer and repeated). Polypropylene 96-well round-bottom natural assay plates (Medos) were used. An amount equal to 50 μL each of competing compound, radioactive ligand, and cell membrane were added successively to give a total assay volume of 150 μL, and the assay was incubated at room temperature for 1 h with shaking. The assay was harvested onto GF/B filtermats (Perkin-Elmer Life Sciences) and pretreated with 0.6% PEI, using 3 × 0.8 mL/well of 20 mM HEPES pH 7.4; 125 mM NaCl at 4 °C. Filtermats were dried, followed by the addition of 9 mL betaplate scintillant and dispersed. The bags were then sealed and counted on a Microbeta counter fitted with six detectors. Each well was counted for 1 min. Data were analyzed using GraphPad Prism software.

NMR Spectroscopy. Samples for NMR contained ∼2 mM peptide in either ^2H_2O or 90% H_2O/10% ^2H_2O at pH 3.5. TOCSY, NOESY, DQF−COSY, and ECOSY spectra were acquired on a Bruker ARX 500 MHz, Bruker ARX 600 MHz, or AVANCE 750 MHz spectrometer with a shielded gradient unit. Spectra were acquired between 281 and 298 K and referenced to internal sodium 2,2-dimethyl-2-silapentane-5-sulfonate. The temperature was maintained within ± 0.1 K, using a BT V2000 control unit and a Bruker BCU refrigeration unit. NOESY spectra were acquired with 200, 250, and 350 ms mixing times, and TOCSY were acquired with an 80 ms mixing time. Water suppression was achieved using a modified WATERGATE[29] sequence. Spectra were acquired with 4096 data points in the F2 dimension and 512 in the F1 dimension and multiplied with squared sine bell functions shifted by 90°. The data t_1 dimension was zero-filled to 1024 real data points.

Information on slowly exchanging amide protons was obtained by acquisition of a series of 1D spectra upon dissolution of a fully protonated peptide in ^2H_2O. $^3J_{HN-H}\alpha$ coupling constants were measured from the DQF−COSY spectrum recorded at 290 K. $^3J_H\alpha$-Hβ coupling constants were determined from the ECOSY spectrum recorded at 295 K in ^2H_2O and transformed over the relevant spectral region to 8192 by 1024 data points.

Structure Calculations. Distance restraints were derived from the 200 ms NOESY spectrum using the program DYANA.[30] Backbone dihedral restraints of −120 ± 40° were applied for $^3J_{HN-H}\alpha > 8.5$ Hz and −60 ± 30° for $^3J_{HN-H}\alpha < 5.0$. Additional ϕ angle restraints (−100 ± 80°) were applied where the intraresidue dαN(i,i) NOE was clearly weaker than the sequential dαN(i,i + 1) NOE. Stereospecific assignments of β-methylene protons and χ1 dihedral angles were derived from $^3J_H\alpha$-Hβ coupling constants, measured from ECOSY spectra, in combination with NOE peak intensities from the 150 ms NOESY spectra. The χ1 angles were restrained to either 60 ± 30°, 180 ± 30°, or −60 ± 30°.

Preliminary structures of **1** were calculated using a torsion angle simulated annealing protocol within DYANA. Final structures were calculated using simulated annealing and energy minimization protocols within CNS version 1.1.[31] The starting structures were generated using random (ϕ, ψ) dihedral angles and were energy-minimized to produce structures with the correct local geometry. A set of 50 structures was generated by a torsion angle simulated annealing protocol as described

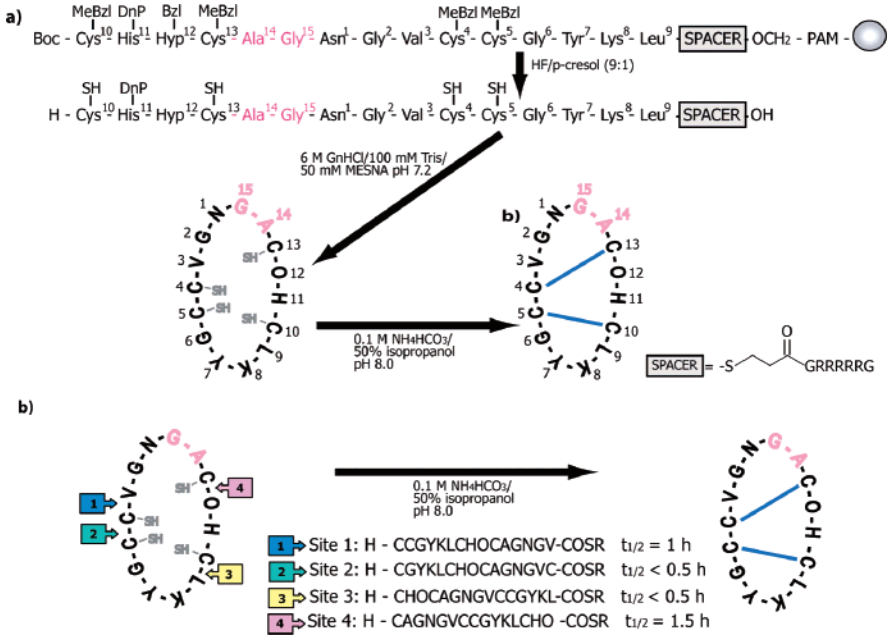

Figure 2. (a) Synthetic strategy for the preparation of **1**. The linear, reduced peptide is synthesized upon resin beads connected by a polyarginine "spacer." Upon HF cleavage, the peptide is removed from the resin. During cyclization, the spacer is removed and the C- and N-termini are connected. Oxidation of the peptide results in the disulfide bonds being formed in the ribbon connectivity shown above. (b) The four possible ligation sites and linear thioester precursor peptides for the synthesis of **1** are shown by the colored arrows. The half-lives for the formation of cyclic peptide from each of the precursors is indicated.

recently for other conotoxins.[23,32] Structures were analyzed using PROMOTIF[33] and PROCHECK-NMR.[34]

Digestion with Endoproteases. Preliminary digestion assays were performed at a 50:1 substrate (peptide)/enzyme ratio for pepsin, trypsin, and proteinase K. For all assays, peptides were incubated with enzyme at 37 °C for either 24 or 48 h and included a positive control, a linear 34-amino acid peptide, corresponding to a truncated form of the bacterial chaperone *Escherichia coli* DnaK 577−610, to ensure an active enzyme was present.[35] All digestion assay data was analyzed by LC/MS chromatography. Trypsin and proteinase K stocks were prepared in 100 mM NH_4HCO_3 buffer (pH 8), and pepsin stocks were prepared in 100 mM acetic/formic acid buffer (pH 2). The trypsin and proteinase K reactions were halted with 0.05% formic acid, and the pepsin reactions were halted with 100 mM NH_4HCO_3. In the preliminary assays, trypsin was the only enzyme that successfully digested MrIA−NH_2. To investigate the effect of the peptide/enzyme ratio on the digestion of these peptides, preliminary assays also included digestions performed at approximately a 5:1 ratio. All trypsin assays were incubated in 100 mM ammonium bicarbonate buffer (pH 8) at 37 °C for the various time points between 0 and 24 h. Additional assays were performed with incubation replicates at a 20:1 substrate/enzyme ratio for 24 h under the same conditions.

Results

Synthesis of 1. We synthesized a cyclic version of MrIA, referred to as **1**, with two residues in a linker (Ala-Gly) joining the ends of the native peptide sequence. The cyclization strategy was designed to minimize side reactions and the number of intermediate isolation steps that could potentially reduce yields. The synthetic scheme incorporating intramolecular native chemical ligation is shown in Figure 2 and involves an intramolecular thioester exchange between an N-terminal cysteine residue and a C-terminal thioester incorporated as part of a spacer moiety linked to the resin. The reaction product spontaneously rearranges to yield a native peptide bond in mild basic aqueous buffer.[36,37] Furthermore, the presence of multiple cysteine residues accelerates the cyclization process through a thia-zip mechanism,[38] where the distant N-terminal cysteine residue is brought into proximity of the C-terminus via successive, reversible interactions with internal cysteines.

A hydrophilic tail consisting of five arginine residues was incorporated into the thioester spacer to assist peptide solubility prior to cyclization.[39] Peptides were assembled using Boc in situ neutralization chemistry and cleaved from the resin using HF/*p*-cresol (9:1 V:V) for 2 h at 0 °C. As the thioester spacer is not compatible with thiol treatment on-resin, the His(Dnp) group was not removed with 2-mercaptoethanol prior to cleavage. Thus, the His(Dnp) group was retained following cleavage and removed by thiolysis during the cyclization step. Cyclization was performed in 6 M guanidine hydrochloride; 100 mM Tris HCl buffer, pH 7.2, containing 50 mM MESNA as a thiol additive to improve the rate of cyclization through a transthioesterification process.[40] Furthermore, the addition of MESNA as a water soluble auxiliary thiol had the advantage of effecting the removal of the His(Dnp) group.

The target analogue contains four cysteine residues, which gives rise to four possible ligation sites that could result in the same cyclic peptide product, as shown in Figure 2. The cyclization efficiency of each of the linear thioester precursors was determined with analytical RP-HPLC. Although each of the four linear thioester precursors yielded the correct cyclized product after ligation, significant differences were observed in the rate of cyclization. At site **1** (Cys-Val) and site **4** (Cys-Hyp), cyclization proceeded at a slower rate, presumably the result of steric hindrance of the C-terminal Val and Hyp residues. Cyclization at sites **2** (Cys-Cys) and **3** (Cys-Leu) proceeded most rapidly, with all starting material converted to a cyclic peptide within 30 min. This trend follows previously observed rates for intermolecular native chemical ligation, where the slowest rates of ligation occur between Cys-Pro and Cys-Val[41]. Disulfide bonds were formed in a separate oxidation step by stirring the reduced cyclic peptide in 0.1 M NH_4HCO_3, pH 8.0, in 50%

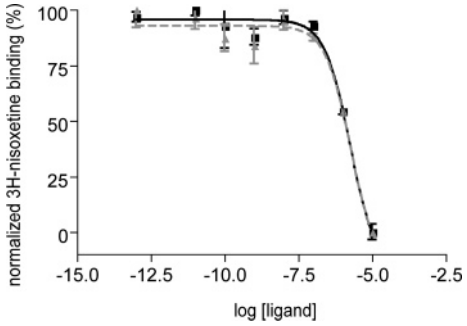

Figure 3. Specific binding of χ-conotoxin MrIA$-NH_2$ (represented by black squares) and **1** (represented by gray triangles) against ^{3}H-nisoxetine in Cos7-hNET membrane. The average log EC_{50} of MrIA$-NH_2$ was -5.74 ± 0.05 M, and the average log EC_{50} of **1** was -5.86 ± 0.28 M ($n = 9$ and $n = 7$, respectively).

2-propanol. Oxidation proceeded cleanly with the formation of one major isomer within 4 h. The cyclic oxidized peptide was isolated by preparative RP-HPLC. The purity of the final product was confirmed by analysis on two different HPLC solvent systems; the chromatographic data are supplied as Supporting Information.

Radiolabeled Ligand Displacement Studies. Displacement of radiolabeled ^{3}H-nisoxetine by **1** and MrIA$-NH_2$ was conducted to determine their binding to expressed human NET in Cos7 cells, as shown in Figure 3. Membranes were incubated with [^{3}H] nisoxetine in the absence or presence of peptide. The average log EC_{50} of MrIA$-NH_2$ was -5.74 ± 0.05, and the average log EC_{50} of **1** was -5.86 ± 0.28 ($n = 9$ and $n = 7$, respectively).

NMR Spectroscopy. Compound **1** gave good quality NMR spectra in aqueous solution between pH 2−5.6 and temperatures in the range 281−298 K. No significant chemical shift changes were observed over the measured pH range, and pH 3.5 was chosen for further analysis based on an expected minimum in the amide exchange rate.[42] Assignments were achieved using the sequential assignment strategy,[42] and a complete cycle of $\alpha H_i - NH_{(i+1)}$ sequential connectivities was observed for the entire sequence with the exception of Hyp12, where instead NOEs were observed between His11 and the Hyp12 side chain protons, thereby completing the sequential connectivity. The amide regions of the TOCSY and NOESY spectra with the resonance assignments annotated are provided as Supporting Information. The presence of a strong NOE between the αH of His11 and the δH protons of Hyp12 suggested that the hydroxyproline residue was in a trans conformation, which is consistent with the conformation of the native peptide.[23]

The αH secondary shifts (i.e., the differences between the observed and random coil αH shift), NOE connectivities, and HN−Hα and Hα−Hβ coupling data for the major conformation are summarized in Figure 4. The positive secondary shifts for the αH resonances of residues 2−5 and 9−12 suggest that **1** contains a small β-sheet structure involving two β-strands. This assumption is supported by the coupling constant data, as residues 3−5 and 9−11 have large $^3J_{HN-H\alpha}$ coupling constants (≥8.5 Hz), indicative of extended structures. Slowly exchanging protons from Gly2, Val3, Cys4, Leu9, and Cys13 were detected 1 h after dissolution of the peptide in ^2H_2O, with Val3 being the only amide signal detectable after 4 h. This observation provides evidence of protection of these protons from the solvent and thereby indicates a well-defined secondary structure of the cyclic molecule. By contrast, in the native peptide, only amide protons from Val3, Cys4, and Leu9 were detectable after 1 h, and all of the amide protons were fully exchanged within 4 h. A summary of the slow exchange data is provided as Supporting Information.

A total of 85 distance restraints (55 sequential, 8 medium, and 22 long range) were obtained from the NOE data. Seven ϕ angle restraints ($-120 \pm 30°$ for Asn1, Val3, Cys4, Leu9, Cys10, and His11 and $-120 \pm 15°$ for Cys5) were derived from the DQF−COSY spectrum. Three additional ϕ angle restraints were applied ($-100 \pm 80°$ for Tyr7 and Ala14 and $50 \pm 40°$ for Lys8) based on NOE intensities and coupling constants.[43] A χ_1-dihedral angle ($-60 \pm 30°$) for Asn1 was derived from the ECOSY spectrum and NOE intensities. The β-protons for this residue were also stereospecifically assigned.

A family of 50 structures was calculated using a torsion angle dynamics protocol within CNS[31] using procedures described

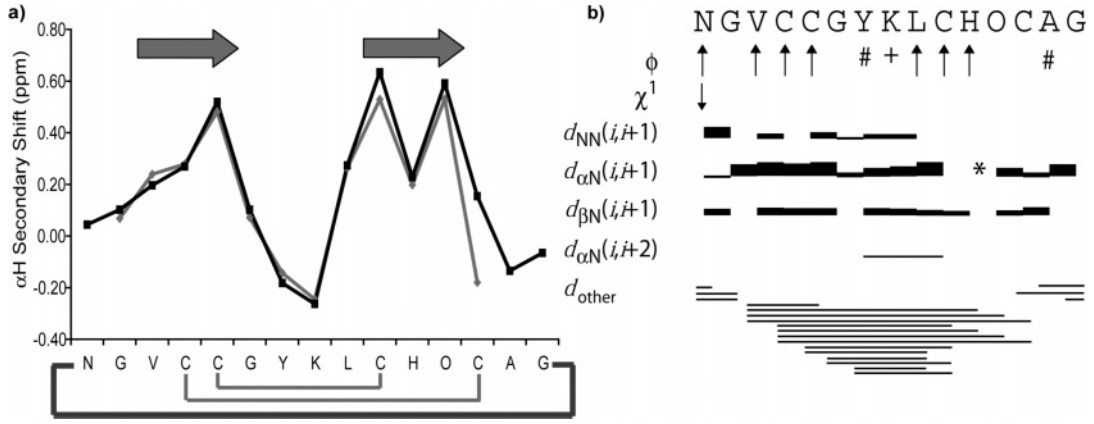

Figure 4. (a) Secondary shifts of **1** and the native peptide, MrIA$-NH_2$. The secondary shifts were determined by subtracting the random coil shift[58] from the experimental αH shift. Compound **1** is represented in black and MrIA$-NH_2$ is shown in gray. No data for residue Asn[1] of MrIA$-NH_2$ were available from the recorded spectra. The light gray lines between the cysteine residues in the sequence on the *x*-axis show the disulfide connectivities of MrIA$-NH_2$ and **1**, and the cyclized backbone of **1** is represented by the dark gray line between the residues of the termini. The β-sheet secondary structures of both MrIA$-NH_2$ and **1** are illustrated by the block arrows between residues 3−5 and 10−12. (b) Summary of the sequential and medium to long-range NOE information and the coupling constants for **1**. For the ϕ angles, arrows pointing up and arrows pointing down represent coupling constants of ≥8.5 Hz and ≤5.0 Hz, respectively. Hash symbols (#) represent dihedral angle restraints of $-100 \pm 80°$ (determined from the NOESY spectrum) and + symbols represent dihedral angle constraints of $50 \pm 40°$. One χ-dihedral angle was incorporated in the structure calculations and is represented as an arrow pointing down for an angle restraint of $-60 \pm 30°$. The height of the bars indicates the relative NOE strength (strong, medium, or weak). In the $d_\alpha N_{(i,i+1)}$ line, an asterisk represents an overlap in the amide protons for residues 10 and 11. For the d_{other} line of the diagram, solid lines represent one or more NOEs between any protons of the starting and ending point residues.

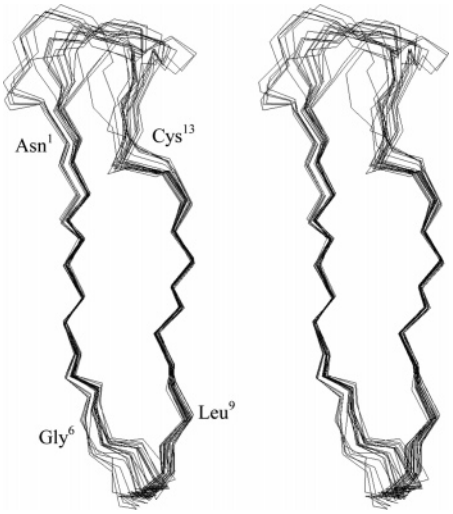

Figure 5. Backbone superposition of the representative ensemble of **1** structures (in stereo), superimposed over residues 3−5 and 10−12, displaying the apparent flexible turn region (Gly^6-Leu^9), linking the strands of the β-hairpin as well as the more flexible linker turn region (Asn^1-Cys^{13}) that joins the termini of the peptide.

previously.[44] The 20 lowest energy structures were chosen as the final ensemble, which had a pairwise RMSD of 0.96 Å over the backbone and 1.69 Å for all heavy atoms. The structures have no NOE violations greater than 0.3 Å and no dihedral violations greater than 3°. Residues 3−12 of **1** form a β-hairpin with the strands (residues 3−5 and 10−12) connected in part by an inverse γ-turn between residues 6−8. If the β-strand regions of the structures (residues 3−5 and 10−12) are overlayed, the RMSD decreases to 0.23 ± 0.13 Å, indicating that there is some disorder in the turn regions (residues 6−9, 14, and 15) of the structure.

Figure 5 shows the backbone superposition of the representative ensemble (in stereo), displaying the apparently flexible native turn region (Gly6-Leu9) as well as the linker turn region (Ala14-Gly15). The structures have good covalent geometry, indicated by small deviations from ideal bond lengths and bond angles. Relevant geometric and energetic statistics, as well as Ramachandran plot statistics, are given in Table 1. All hydrogen bonds corresponding to slowly exchanging amide protons, except Val3 and Leu9, were verified in the structures using MOLMOL[45] (e.g., Cys4 HN and His11 O, Gly2 HN and Cys13 O, and Cys13 HN and Gly2 O).

The structures were calculated using the same disulfide connectivity as the native peptide (i.e., ribbon connectivity). The disulfide bond between Cys4-Cys13 has a right-handed hook conformation in 10/20 structures, and the disulfide bond between Cys5-Cys10 has a short right-handed hook conformation in 19/20 structures. Structures were also calculated for the alternative, globular connectivity to confirm the formation of the correct isomer.[23,44] As shown in Table 1, both the average NOE energy and dihedral angle energy values for the globular isomer of **1** increased dramatically to 94.5 kcal mol^{-1} and 83.6 kcal mol^{-1}, respectively, relative to the ribbon connectivity of the peptide with an average NOE energy of 4.8 kcal mol^{-1} and dihedral angle energy of 0.4 kcal mol^{-1}, confirming that **1** adopts a native ribbon fold.

Enzymatic Stability. Enzymatic digestion assays were performed with MrIA−NH_2 and **1** to compare the resistance to proteolysis of the native and cyclized versions. Preliminary assays included incubating the peptides with pepsin, trypsin, and proteinase K for 24 h at 37 °C. A linear peptide was used as a positive control for all assays and, in all cases, was completely digested (i.e., <5% intact peptide remaining) after 15 min of incubation (data not shown). Pepsin and proteinase K failed to significantly digest either MrIA−NH_2 or **1** within 24 h. However, trypsin successfully digested linear MrIA−NH_2 within 24 h at a 20:1 ratio (peptide/trypsin), as shown in Figure 6. The trypsin cleavage site is located in the turn region of MrIA−NH_2 and **1** at residue 8. Less than 55% of intact MrIA−NH_2 remained intact after 24 h compared to 97% of intact **1** remaining, clearly demonstrating an increase in the trypsin stability of the cyclized version of the peptide. Furthermore, because it contains no termini, the cyclic version is by definition resistant to exoproteases.

Table 1. Geometric and Energetic Statistics for Families of 20 Structures of **1** Calculated with χ-Conopeptide "Ribbon" and α-Conopeptide "Globular" Disulfide Connectivities[a]

experimental restraints	ribbon	globular
sequential NOEs	55	55
medium range NOEs	8	8
long-range NOEs	22	22
dihedral angles	11	11
Mean RMSDs from Experimental Restraints		
NOE distances (Å)	0.03 ± 0.0055	0.15 ± 0.0219
dihedral angles (°)	0.72 ± 0.240	4.57 ± 1.0122
Mean RMSDs from Idealized Covalent Geometry		
bonds (Å)	0.0039 ± 0.0003	0.0109 ± 0.0014
angles (°)	0.54 ± 0.04	1.12 ± 0.05
impropers (°)	0.44 ± 0.03	1.03 ± 0.13
Mean Energies (kcal mol^{-1})		
$E_{NOE}{}^C$	4.80 ± 1.55	94.50 ± 27.47
$E_{DIH}{}^C$	0.35 ± 0.20	83.58 ± 8.25
E_{bond}	3.03 ± 0.47	24.10 ± 5.67
E_{angle}	16.12 ± 2.52	63.34 ± 5.98
$E_{improper}$	3.08 ± 0.37	17.29 ± 3.80
E_{VDW}	−24.91 ± 4.42	37.22 ± 15.95
Atomic RMSDs[b] (Å)		
backbone atoms	0.96 ± 0.52	1.44 ± 0.77
heavy atoms	1.69 ± 0.44	2.35 ± 0.85
backbone atoms (residues 3−5 and 10−12)	0.23 ± 0.13	0.65 ± 0.48
heavy atoms (residues 3−5 and 10−12)	1.06 ± 0.36	2.35 ± 0.85
Ramachandran Statistics[c] (%)		
residues in most favored regions	77.9	55.6
residues in additional allowed regions	22.1	43.1
residues in generously allowed regions	0.0	1.2

[a] The values in the table are the mean ± S. D. [b] Atomic RMSDs are the pairwise root-mean-square differences for the family of structures. [c] Procheck NMR was used to calculate the Ramachandran statistics for residues 1−13.

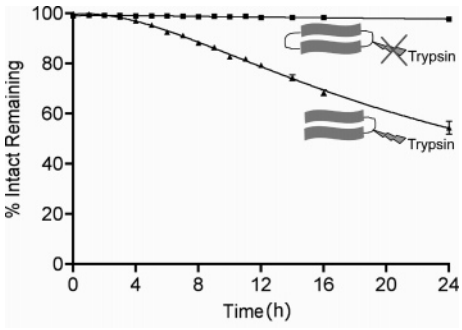

Figure 6. Trypsin digest of MrIA−NH_2 and **1**. MrIA−NH_2 is represented by triangles and **1** is represented by squares. Peptide (i.e., substrate) and trypsin (i.e., enzyme) were incubated in a 20:1 ratio. A positive control, DnaK-f2, which contains several lysines in its sequence (i.e., KGEDKAAEIAKMQELAQVSQKLMEIAQQQHAQQQ) was completely digested by trypsin (i.e., <5% remaining) within 15 min of incubation (data not shown).

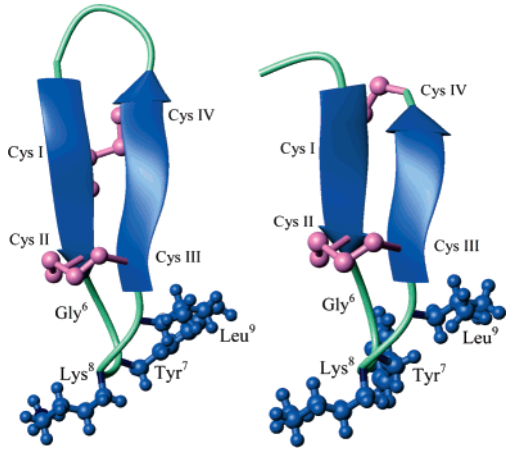

Figure 7. Ribbon representation of **1** (left) and linear MrIA−NH_2 (right). An overlay of the sheet regions of **1** and MrIA−NH_2 has a RMSD of 0.18 Å, indicating very similar structures. Disulfide bonds and the side chains of the residues in the native turn region are shown in a ball-and-stick representation. The structures were visualized using MOLMOL.[45] Note that the Cys I−IV disulfide bond is on the opposite side of the β-sheet to the Cys II−III disulfide bond and is partially obscured in the view shown.

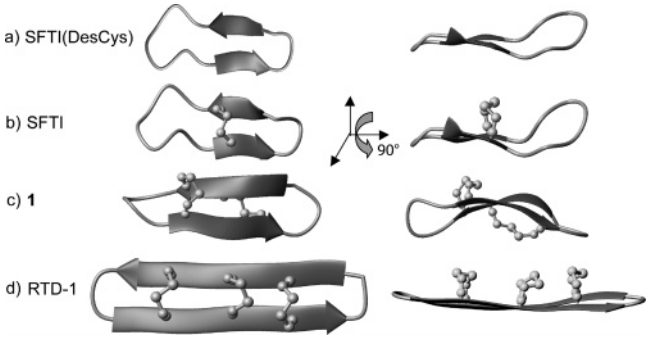

Figure 8. Comparison of the ribbon representations of (from top to bottom) SFTI-1(DesCys) (without a disulfide bond),[59] SFTI (native),[55] **1**, and RTD-1[53] showing the various topologies of β-hairpin peptides containing cyclized backbones, all with different biological activities.

Discussion

In the current study we have shown that cyclizing the backbone of MrIA leads to an increase in enzymatic stability relative to the native peptide, thereby improving its potential as a drug lead. Compound **1** was synthesized without selective protection of the cysteine residues and oxidized efficiently to produce mainly the native ribbon isomer. The cyclic version of MrIA retains essentially identical activity and structure to the native peptide. Figure 7 shows that the global folds of the two peptides are almost identical, overlaying in the β-hairpin region with an RMSD of 0.18 Å. Furthermore, a comparison of **1** with MrIA−NH_2 reveals a slightly lower RMSD over residues 1−13 for the structural ensemble of the cyclic version, indicating that cyclization of MrIA produces a more well-defined structure. In essence, cyclization produces a molecule with identical activity and structure but improved resistance to proteolysis.

The residues previously found to be important for biological activity of MrIA include Tyr7, Lys8, Leu9, and to a lesser extent His11.[12] As shown in Figure 7, these residues are located in the turn connecting the β-strands, and their side chain orientations are generally conserved between the cyclic and native form. The side chain orientation of Tyr7 is somewhat different between the two forms, but this likely reflects a lack of NOE restraints in this region rather than a conformational difference. An alanine scan performed by Sharpe et al.[12] indicated that Gly6 has a significant effect on the structure and was proposed to have a role in the orientating of other residues for interaction with the NET. This residue remains relatively unchanged in conformation in **1** relative to the native peptide, consistent with the maintenance of activity in **1**.

Incubation of **1** with trypsin revealed that it was less susceptible to proteolysis than MrIA−NH_2, despite the potential cleavage site being distant from the site of cyclization. The structures of the cyclic and acyclic forms of MrIA are very similar, making this resistance to proteolysis a somewhat surprising finding. This difference in susceptibility to proteolysis adjacent to Lys8 is not due to differences in screening of the active site residue from external interactions; as in both cases, this residue is relatively solvent exposed. There is a difference between the amide exchange rates of the cyclic and acyclic peptides, with the cyclic form having slower exchange rates for several residues, indicating a general decrease in flexibility relative to the acyclic form. The small size of MrIA and **1** means that not all amides are solvent shielded or hydrogen bonded, so it is not surprising that not all amides experience differences in exchange rates, but it is reasonable to speculate that cyclization causes a general tightening of the structure. NMR relaxation studies would be necessary to confirm this hypothesis. The likely differences in flexibility of the cyclic and acyclic forms may have significant implications for stability, as potential cleavage sites within proteins are more susceptible to cleavage by proteases if they are in flexible regions.[46] Similar results to those observed in the current study with MrIA have been observed for cyclic versions of α-conotoxin MII, where cyclization was shown to result in increased resistance to proteolysis and a decrease in amide exchange rates.[27] Furthermore, decreased amide exchange rates have also been reported for cyclic relative to linear versions of other proteins, including the plant cyclotides[47] and the replicative helicase DnaB from *E. coli*,[48] and rigidification appears to be a general phenomenon associated with cyclization.

We have now exemplified cyclization as a tool for improving stability for members from both the α- and χ-conotoxins, indicating that this approach may be applicable to a range of conotoxin classes. However, the number of residues required to span the N- and C-termini is dependent on the structure of the native peptide. The different structures of the α- and χ-conotoxins mean that significant differences are observed in the number of residues required in the "linker" region between the termini. The three-dimensional structures of α-conotoxins are characterized by a helical region and a globular connectivity of the disulfide bonds[49] in contrast to the β-hairpin structure and ribbon disulfide connectivity of the χ-conotoxins. At least six residues are necessary to span the distance between the termini of the α-conotoxin MII and maintain structure and activity at the nicotinic acetylcholine receptor.[27] By contrast, the β-hairpin structure of MrIA[23] facilitates the cyclization process, with only two residues required to span the termini.

Synthetic engineered cyclic conotoxins have some parallels to disulfide-rich peptides found in nature. Over recent years, an increasing number of peptides with cyclic backbones have been isolated from a wide range of sources, including plants, bacteria, and animals.[50] Examples include the plant cyclotides,[51] RTD-1 (rhesus theta defensin 1),[52,53] and the sunflower trypsin inhibitor, SFTI-1.[54,55] The latter two peptides have two antiparallel β-strands joined at both ends in the circular backbone. A comparison of the structures of a disulfide-deficient SFTI-1-mutant, native SFTI-1, **1**, and native RTD-1 is given in Figure 8 to illustrate a series of cyclic peptides with increasing disulfide

cross-linking. Interestingly, a comparison of the disulfide bonds for RTD-1 and **1** reveals a significant difference in topology: RTD-1 contains three disulfide bonds all on one side of the peptide (in a laddered arrangement) versus **1** with two disulfide bonds on opposing sides of the molecule. Compound **1** thus represents a new topology of small β-hairpin peptides containing circular backbones. The adjacent cysteines (Cys1 and Cys2) in **1** are likely to favor the different topology of **1** compared to that of RTD-1, where the cysteine residues are separated by at least one residue. In contrast to the structures of **1** where the majority of the flexibility is in the turns connecting the β-strands, RTD-1 contains a flexible β-sheet. Interestingly, even though it contains fewer disulfide bonds than RTD-1, SFTI-1 is more rigid due to its extensive hydrogen bonding network.[55]

Tam et al.[56] have reported synthetic cyclic derivatives of the 18-residue antimicrobial peptide tachyplesin. They showed that cyclic structures are useful in the design of antimicrobial peptides and that an increase in the conformational rigidity brought about by an increasing number of disulfide bonds may confer membranolytic selectivity that disassociates antimicrobial activity from haemolytic activity. In other words, cyclization and disulfide stabilization can have advantages in selecting for desired pharmacological effects versus side-effects. Among the structures synthesized were cyclic tachyplesin derivatives with two or three disulfide bonds. The structure of the two-disulfide derivative, which is most analogous to **1**, was modeled as a "laddered" cystine framework with both disulfide bonds on one side of the structure. It would be interesting to determine the experimental structure of this molecule for comparison with the "opposite side" disulfide structure of **1** determined here. Retrocyclin, a synthetic cyclic peptide that has potent anti-HIV activity, has similarly been modeled as a cysteine-laddered framework.[52]

It is interesting to compare **1** with the cyclotides, a group of naturally occurring tri-disulfide cyclic plant peptides.[51] In contrast to **1**, the structures of cyclotides are very well defined due to their cystine knot motif, in which two of the disulfide bonds form an embedded ring completed by the backbone segments connecting the cysteine residues, while the third disulfide bond threads through this ring to form the knot.[57] The cross-bracing arrangement of the disulfide-bonded core creates an exceptionally stable knot and results in a more rigid structure than either **1** or RTD-1, despite their higher proportion of cystine residues.[53]

In summary, χ-conotoxin MrIA has been backbone-cyclized with a two-residue linker, and the cyclic derivative maintains the fold of the native peptide and activity at the NET. Resistance to proteolysis of MrIA by trypsin was significantly improved upon cyclization, despite the cleavage site not being located near the cyclization site. In the past, cyclization has been used mainly for the stabilization of small (<10 amino acid) linear peptides, but the current study shows that it is more generally applicable to well-folded disulfide-containing peptides as a potential route to improving their therapeutic applications.

Acknowledgment. D.J.C. and P.F.A. are Senior Research Affiliates of the Australian Research Council (ARC) Special Research Centre for Functional and Applied Genomics, which provided infrastructure support for the work in this project. D.J.C. is an ARC Professorial Fellow. N.L.D. is an NHMRC Industry Fellow. E.S.L. and C.J.A. acknowledge ARC support. The authors thank Elka Palant, Xenome, for providing assay support and Alun Jones, Institute for Molecular Bioscience, for providing mass spectrometry support. This work was supported by a grant from the ARC.

Supporting Information Available: A table including the purities of MrIA and **1**, determined by two different HPLC systems, a TOCSY and a NOESY sequential walk, and a table including the slow exchange protons of MrIA and **1** used in this work. This material is available free of charge via the Internet at http://pubs.acs.org.

References

(1) Terlau, H.; Olivera, B. M. Conus venoms: A rich source of novel ion channel-targeted peptides. *Physiol. Rev.* **2004**, *84*, 41−68.
(2) Adams, D. J.; Alewood, P. F.; Craik, D. J.; Drinkwater, R. D.; Lewis, R. J. Conotoxins and their potential pharmaceutical applications. *Drug Dev. Res.* **1999**, *46*, 219−234.
(3) Olivera, B. M.; Cruzab, L. J. Conotoxins, in retrospect. *Toxicon* **2001**, *39*, 7−14.
(4) Livett, B. G.; Gayler, K. R.; Khalil, Z. Drugs from the sea: conopeptides as potential therapeutics. *Curr. Med. Chem.* **2004**, *11*, 1715−1723.
(5) Staats, P. S.; Yearwood, T.; Charapata, S. G.; Presley, R. W.; Wallace, M. S.; Byas-Smith, M.; Fisher, R.; Bryce, D. A.; Mangieri, E. A.; Luther, R. R.; Mayo, M.; McGuire, D.; Ellis, D. Intrathecal ziconotide in the treatment of refractory pain in patients with cancer or AIDS: a randomized controlled trial. *JAMA, J. Am. Med. Assoc.* **2004**, *291*, 63−70.
(6) Arias, H. R.; Blanton, M. P. Alpha-conotoxins. *Int. J. Biochem. Cell Biol.* **2000**, *32*, 1017−1028.
(7) Nielsen, K. J.; Thomas, L.; Lewis, R. J.; Alewood, P. F.; Craik, D. J. A consensus structure for omega-conotoxins with different selectivities for voltage-sensitive calcium channel subtypes: comparison of MVIIA, SVIB, and SNX-202. *J. Mol. Biol.* **1996**, *263*, 297−310.
(8) Dutton, J. L.; Craik, D. J. α-Conotoxins: nicotinic acetylcholine receptor antagonists as pharmacological tools and potential drug leads. *Curr. Med. Chem.* **2001**, *8*, 327−344.
(9) Garber, K. Peptide leads new class of chronic pain drugs. *Nat. Biotechnol.* **2005**, *23*, 399.
(10) Wermeling, D. P.; Berger, J. R. Ziconotide infusion for severe chronic pain: case series of patients with neuropathic pain. *Pharmacotherapy* **2006**, *26*, 395−402.
(11) Sharpe, I. A.; Gehrmann, J.; Loughnan, M. L.; Thomas, L.; Adams, D. A.; Atkins, A.; Palant, E.; Craik, D. J.; Adams, D. J.; Alewood, P. F.; Lewis, R. J. Two new classes of conopeptides inhibit the α1-adrenoceptor and noradrenaline transporter. *Nat. Neurosci.* **2001**, *4*, 902−907.
(12) Sharpe, I. A.; Palant, E.; Schroeder, C. I.; Kaye, D. M.; Adams, D. J.; Alewood, P. F.; Lewis, R. J. Inhibition of the norepinephrine transporter by the venom peptide chi-MrIA. Site of action, Na^+ dependence, and structure−activity relationship. *J. Biol. Chem.* **2003**, *278*, 40317−40323.
(13) Nielsen, C. K.; Lewis, R. J.; Alewood, D.; Drinkwater, R.; Palant, E.; Patterson, M.; Yaksh, T. L.; McCumber, D.; Smith, M. T. Anti-allodynic efficacy of the chi-conopeptide, Xen2174, in rats with neuropathic pain. *Pain* **2005**, *118*, 112−124.
(14) Brunello, N.; Mendlewicz, J.; Kasper, S.; Leonard, B.; Montgomery, S.; Nelson, J.; Paykel, E.; Versiani, M.; Racagni, G. The role of noradrenaline and selective noradrenaline reuptake inhibition in depression. *Eur. Neuropsychopharmacol.* **2002**, *12*, 461−475.
(15) Tanaka, M.; Yoshida, M.; Emoto, H.; Ishii, H. Noradrenaline systems in the hypothalamus, amygdala and locus coeruleus are involved in the provocation of anxiety: basic studies. *Eur. J. Pharmacol.* **2000**, *405*, 397−406.
(16) Drummond, P. D. Noradrenaline increases hyperalgesia to heat in skin sensitized by capsaicin. *Pain* **1995**, *60*, 311−315.
(17) Furst, S. Transmitters involved in antinociception in the spinal cord. *Brain Res. Bull.* **1999**, *48*, 129−141.
(18) Arnsten, A. F. Adrenergic targets for the treatment of cognitive deficits in schizophrenia. *Psychopharmacology (Berlin)* **2004**, *174*, 25−31.
(19) Ressler, K. J.; Nemeroff, C. B. Role of norepinephrine in the pathophysiology and treatment of mood disorders. *Biol. Psychiatry* **1999**, *46*, 1219−1233.
(20) McIntosh, J. M.; Corpuz, G. O.; Layer, R. T.; Garrett, J. E.; Wagstaff, J. D.; Bulaj, G.; Vyazovkina, A.; Yoshikami, D.; Cruz, L. J.; Olivera, B. M. Isolation and characterization of a novel conus peptide with apparent antinociceptive activity. *J. Biol. Chem.* **2000**, *275*, 32391−32397.
(21) Balaji, R. A.; Ohtake, A.; Sato, K.; Gopalakrishnakone, P.; Kini, R. M.; Seow, K. T.; Bay, B. H. λ-Conotoxins, a new family of conotoxins with unique disulfide pattern and protein folding. Isolation and characterization from the venom of Conus marmoreus. *J. Biol. Chem.* **2000**, *275*, 39516−39522.

(22) Gehrmann, J.; Alewood, P. F.; Craik, D. J. Structure determination of the three disulfide bond isomers for α-conotoxin GI: A model for the role of disulfide bonds in structural stability. *J. Mol. Biol.* **1998**, *278*, 401−415.
(23) Nilsson, K. P.; Lovelace, E. S.; Caesar, C. E.; Tynngard, N.; Alewood, P. F.; Johansson, H. M.; Sharpe, I. A.; Lewis, R. J.; Daly, N. L.; Craik, D. J. Solution structure of chi-conopeptide MrIA, a modulator of the human norepinephrine transporter. *Biopolymers* **2005**, *80*, 815−823.
(24) Iwai, H.; Pluckthun, A. Circular *β*-lactamase: stability enhancement by cyclizing the backbone. *FEBS Lett.* **1999**, *459*, 166−172.
(25) Williams, N. K.; Prosselkov, P.; Liepinsh, E.; Line, I.; Sharipo, A.; Littler, D. R.; Curmi, P. M.; Otting, G.; Dixon, N. E. In vivo protein cyclization promoted by a circularly permuted *Synechocystis* sp. PCC6803 DnaB mini-intein. *J. Biol. Chem.* **2002**, *277*, 7790−7798.
(26) Iwai, H.; Lingel, A.; Pluckthun, A. Cyclic green fluorescent protein produced in vivo using an artificially split PI-PfuI intein from *Pyrococcus furiosus*. *J. Biol. Chem.* **2001**, *276*, 16548−16554.
(27) Clark, R. J.; Fischer, H.; Dempster, L.; Daly, N. L.; Rosengren, K. J.; Nevin, S. T.; Meunier, F. A.; Adams, D. J.; Craik, D. J. Engineering stable peptide toxins by means of backbone cyclization: stabilization of the α-conotoxin MII. *Proc. Natl. Acad. Sci. U.S.A.* **2005**, *102*, 13767−13772.
(28) Schnolzer, M.; Alewood, P.; Jones, A.; Alewood, D.; Kent, S. B. In situ neutralization in Boc-chemistry solid phase peptide synthesis. Rapid, high yield assembly of difficult sequences. *Int. J. Pept. Protein Res.* **1992**, *40*, 180−193.
(29) Piotto, M.; Saudek, V.; Sklenar, V. Gradient-tailored excitation for single-quantum NMR spectroscopy of aqueous solutions. *J. Biomol. NMR* **1992**, *2*, 661−665.
(30) Güntert, P.; Mumenthaler, C.; Wüthrich, K. Torsion angle dynamics for NMR structure calculation with the new program DYANA. *J. Mol. Biol.* **1997**, *273*, 283−298.
(31) Brunger, A. T.; Adams, P. D.; Rice, L. M. New applications of simulated annealing in X-ray crystallography and solution NMR. *Structure* **1997**, *5*, 325−336.
(32) Daly, N. L.; Ekberg, J. A.; Thomas, L.; Adams, D. J.; Lewis, R. J.; Craik, D. J. Structures of *μ*-*O*-conotoxins from Conus marmoreus. Inhibitors of tetrodotoxin (TTX)-sensitive and TTX-resistant sodium channels in mammalian sensory neurons. *J. Biol. Chem.* **2004**, *279*, 25774−25782.
(33) Hutchinson, E. G.; Thornton, J. M. PROMOTIF—A program to identify and analyze structural motifs in proteins. *Protein Sci.* **1996**, *5*, 212−220.
(34) Laskowski, R. A.; Rullmannn, J. A.; MacArthur, M. W.; Kaptein, R.; Thornton, J. M. AQUA and PROCHECK−NMR: programs for checking the quality of protein structures solved by NMR. *J. Biomol. NMR* **1996**, *8*, 477−486.
(35) Colgrave, M. L.; Craik, D. J. Thermal, chemical, and enzymatic stability of the cyclotide kalata B1: the importance of the cyclic cystine knot. *Biochemistry* **2004**, *43*, 5965−5975.
(36) Dawson, P. E.; Muir, T. W.; Clark-Lewis, I.; Kent, S. B. Synthesis of proteins by native chemical ligation. *Science* **1994**, *266*, 776−779.
(37) Tam, J. P.; Lu, Y. A. A biomimetic strategy in the synthesis and fragmentation of cyclic protein. *Protein Sci.* **1998**, *7*, 1583−1592.
(38) Tam, J. P.; Lu, Y. A.; Yu, Q. T. Thia zip reaction for synthesis of large cyclic peptides: Mechanisms and applications. *J. Am. Chem. Soc.* **1999**, *121*, 4316−4324.
(39) Aimoto, S. Polypeptide synthesis by the thioester method. *Biopolymers* **1999**, *51*, 247−265.
(40) Dawson, P. E.; Churchill, M. J.; Ghadiri, M. R.; Kent, S. B. H. Modulation of reactivity in native chemical ligation through the use of thiol additives. *J. Am. Chem. Soc.* **1997**, *119*, 4325−4329.
(41) Hackeng, T. M.; Griffin, J. H.; Dawson, P. E. Protein synthesis by native chemical ligation: expanded scope by using straightforward methodology. *Proc. Natl. Acad. Sci. U.S.A.* **1999**, *96*, 10068−10073.
(42) Wüthrich, K. *NMR of proteins and nucleic acids*; Wiley-Interscience: New York, 1986.
(43) Clubb, R. T.; Ferguson, S. B.; Walsh, C. T.; Wagner, G. Three-dimensional solution structure of *Escherichia coli* periplasmic cyclophilin. *Biochemistry* **1994**, *33*, 2761−2772.
(44) Daly, N. L.; Koltay, A.; Gustafson, K. R.; Boyd, M. R.; Casas-Finet, J. R.; Craik, D. J. Solution structure by NMR of circulin A: a macrocyclic knotted peptide having anti-HIV activity. *J. Mol. Biol.* **1999**, *285*, 333−345.
(45) Koradi, R.; Billeter, M.; Wuthrich, K. MOLMOL: a program for display and analysis of macromolecular structures. *J. Mol. Graphics Modell.* **1986**, *14*, 51−55.
(46) Hubbard, S. J. The structural aspects of limited proteolysis of native proteins. *Biochim. Biophys. Acta* **1998**, *1382*, 191−206.
(47) Daly, N. L.; Craik, D. J. Acyclic permutants of naturally occurring cyclic proteins. Characterization of cystine knot and *β*-sheet formation in the macrocyclic polypeptide kalata B1. *J. Biol. Chem.* **2000**, *275*, 19068−19075.
(48) Williams, N. K.; Liepinsh, E.; Watt, S. J.; Prosselkov, P.; Matthews, J. M.; Attard, P.; Beck, J. L.; Dixon, N. E.; Otting, G. Stabilization of native protein fold by intein-mediated covalent cyclization. *J. Mol. Biol.* **2005**, *346*, 1095−1108.
(49) Millard, E. L.; Daly, N. L.; Craik, D. J. Structure−activity relationships of α-conotoxins targeting neuronal nicotinic acetylcholine receptors. *Eur. J. Biochem.* **2004**, *271*, 2320−2326.
(50) Trabi, M.; Craik, D. J. Circular proteins—no end in sight. *Trends Biochem. Sci.* **2002**, *27*, 132−138.
(51) Craik, D. J.; Daly, N. L.; Bond, T.; Waine, C. Plant cyclotides: A unique family of cyclic and knotted proteins that defines the cyclic cystine knot structural motif. *J. Mol. Biol.* **1999**, *294*, 1327−1336.
(52) Tang, Y. Q.; Yuan, J.; Osapay, G.; Osapay, K.; Tran, D.; Miller, C. J.; Ouellette, A. J.; Selsted, M. E. A cyclic antimicrobial peptide produced in primate leukocytes by the ligation of two truncated α-defensins. *Science* **1999**, *286*, 498−502.
(53) Trabi, M.; Schirra, H. J.; Craik, D. J. Three-dimensional structure of RTD-1, a cyclic antimicrobial defensin from Rhesus macaque leukocytes. *Biochemistry* **2001**, *40*, 4211−4221.
(54) Luckett, S.; Garcia, R. S.; Barker, J. J.; Konarev, A. V.; Shewry, P. R.; Clarke, A. R.; Brady, R. L. High-resolution structure of a potent, cyclic proteinase inhibitor from sunflower seeds. *J. Mol. Biol.* **1999**, *290*, 525−533.
(55) Korsinczky, M. L.; Schirra, H. J.; Rosengren, K. J.; West, J.; Condie, B. A.; Otvos, L.; Anderson, M. A.; Craik, D. J. Solution structures by ^{1}H NMR of the novel cyclic trypsin inhibitor SFTI-1 from sunflower seeds and an acyclic permutant. *J. Mol. Biol.* **2001**, *311*, 579−591.
(56) Tam, J. P.; Wu, C.; Yang, J. L. Membranolytic selectivity of cystine-stabilized cyclic protegrins. *Eur. J. Biochem.* **2000**, *267*, 3289−3300.
(57) Craik, D. J.; Daly, N. L.; Waine, C. The cystine knot motif in toxins and implications for drug design. *Toxicon* **2001**, *39*, 43−60.
(58) Wishart, D. S.; Bigam, C. G.; Yao, J.; Abildgaard, F.; Dyson, H. J.; Oldfield, E.; Markley, J. L.; Sykes, B. D. ^{1}H, ^{13}C, and ^{15}N chemical shift referencing in biomolecular NMR. *J. Biomol. NMR* **1995**, *6*, 135−140.
(59) Korsinczky, M. L.; Clark, R. J.; Craik, D. J. Disulfide bond mutagenesis and the structure and function of the head-to-tail macrocyclic trypsin inhibitor SFTI-1. *Biochemistry* **2005**, *44*, 1145−1153.

JM060299H